Redox, Magnetic, and Structural Properties of 1,3,2-Dithiazolyl Radicals. A Case Study on the Ternary Heterocycle $S_3N_5C_4$

T. M. Barclay,[1a] A. W. Cordes,[1a] N. A. George,[1b] R. C. Haddon,[1c] M. E. Itkis,[1c] M. S. Mashuta,[1d] R. T. Oakley,*[,1b] G. W. Patenaude,[1b] R. W. Reed,[1b] J. F. Richardson,[1d] and H. Zhang[1b]

Contribution from the Department of Chemistry and Biochemistry, University of Arkansas, Fayetteville, Arkansas 72701, Department of Chemistry and Biochemistry, University of Guelph, Guelph, Ontario N1G 2W1, Canada, Department of Chemistry, University of Kentucky, Lexington, Kentucky 40506, and Department of Chemistry, University of Louisville, Louisville, Kentucky 40292

Received September 23, 1997

Abstract: The characterization of the heterocyclic radical 1,2,5-thiadiazolo[3,4-*b*]-1,3,2-dithiazolo[3,4-*b*]pyrazin-2-yl (TDP-DTA) is described. The compound is prepared by treatment of 5,6-dithiolo-1,2,5-thiadiazolo[3,4-*b*]pyrazine with $S_3N_3Cl_3$ and purified by fractional sublimation in vacuo. The results of cyclic voltammetry and ESR analysis of TDP-DTA and related heterocyclic dithiazolyls indicate that the spin distributions and donor/acceptor properties of these radicals are extremely sensitive to the nature of the 4,5-substituents. The crystal structure of TDP-DTA has been determined at two temperatures. At 293 K, the crystals are triclinic, space group $P\bar{1}$, with $a = 4.4456(8)$, $b = 8.407(2)$, $c = 9.671(3)$ Å, $\alpha = 71.34(2)$, $\beta = 89.28(2)$, $\gamma = 87.80(2)°$, $Z = 2$ (for $C_4N_5S_3$); at 150 K the crystals are triclinic, space group $P\bar{1}$, with $a = 7.489(7)$, $b = 9.593(4)$, $c = 10.759(6)$ Å, $\alpha = 65.77(4)$, $\beta = 74.10(6)$, $\gamma = 74.64(6)°$, $Z = 2$ (for $C_8N_{10}S_6$). At 293 K the structure consists of ribbons of TDP-DTA radicals packed in a slipped π-stack arrangement. In the low temperature phase alternate layers of ribbons are shifted laterally to produce arrays of dimers. Within these dimers three long (3.401(5), 3.460(5) and 3.511(5) Å) interannular S---S contacts link the two molecules. A multiple "tectonic plate" slippage mechanism is proposed to account for the interconversion of the two phases. The structural results are discussed in the light of variable temperature magnetic susceptibility measurements.

Introduction

Neutral heterocyclic π-radicals represent versatile building blocks for applications in the field of molecular materials.[2,3] Most work has focused on derivatives of the 1,2,3,5-dithiadiazolyl system **1** (DTDA) and their selenium analogues, with the intent of using them as molecular conductors.[4,5] Their potential as molecular magnets has also been pursued.[6]

In contrast to the DTDA system, the solid-state structures and transport properties of derivatives of the 1,3,2-dithiazolyl ring **2** (DTA) have received relatively little attention, although the radicals themselves have been known for well over a decade.[7,8] In the solid state the 4,5-dicyano derivative forms the simple cofacial dimer **3**.[9] The pyrazine based compound **4** (PDTA) also dimerizes cofacially,[10] but the dimers adopt a stacked dimer structure similar to that observed for many dithiadiazolyls. Surprisingly, and despite its structural resemblance to PDTA, the benzo-derivative **5** (BDTA)[11] associates in a centrosymmetric manner, i.e., **6**, but does not form π-stacks. The trithiatriazapentalenyl radical **7** (TTTA) represents a sharp contrast to the previous examples, in that dimerization is not observed.[12] Instead the crystal structure consists of evenly spaced slipped π-stacks, and thus nominally fulfills the basic

(1) (a) University of Arkansas. (b) University of Guelph. (c) University of Kentucky. (d) University of Louisville.

(2) (a) Banister, A. J.; Rawson, J. M. In *The Chemistry of Inorganic Ring Systems*; Steudel, R., Ed.; Elsevier: Amsterdam, 1992; p 323. (b) Banister, A. J.; Rawson, J. M. *Adv. Hetero. Chem.* **1995**, *62*, 137. (c) Oakley, R. T. Prog. *Inorg. Chem.* **1988**, *36*, 299.

(3) (a) Cordes, A. W.; Haddon, R. C.; Oakley, R. T. In *The Chemistry of Inorganic Ring Systems*; Steudel, R., Ed.; Elsevier: Amsterdam, 1992; p 295. (b) Cordes, A. W.; Haddon, R. C.; Oakley, R. T. *Adv. Mater*. **1994**, *6*, 798.

(4) (a) Haddon, R. C. *Nature (London)* **1975**, *256*, 394. (b) Haddon, R. C. *Aust. J. Chem.* **1975**, *28*, 2343.

(5) (a) Cordes, A. W.; Haddon, R. C.; Oakley, R. T.; Schneemeyer, L. F.; Waszczak, J. V.; Young, K. M.; Zimmerman, N. M. *J. Am. Chem. Soc.* **1991**, *113*, 582. (b) Andrews, M. P.; Cordes, A. W.; Douglass, D. C.; Fleming, R. M.; Glarum, S. H.; Haddon, R. C.; Marsh, P.; Oakley, R. T.; Palstra, T. T. M.; Schneemeyer, L. F.; Trucks, G. W.; Tycko, R.; Waszczak, J. V.; Young, K. M.; Zimmerman, N. M. *J. Am. Chem. Soc.* **1991**, *113*, 3559. (c) Cordes, A. W.; Haddon, R. C.; Hicks, R. G.; Oakley, R. T.; Palstra, T. T. M.; Schneemeyer, L. F.; Waszczak, J. V. *J. Am. Chem. Soc.* **1992**, *114*, 5000. (d) Cordes, A. W.; Haddon, R. C.; Hicks, R. G.; Kennepohl, D. K.; Oakley, R. T.; Schneemeyer, L. F.; Waszczak, J. V. *Inorg. Chem.* **1993**, *32*, 1554. (e) Bryan, C. D.; Cordes, A. W.; Goddard, J. D.; Haddon, R. C.; Hicks, R. G.; Mackinnon, C. D.; Mawhinney, R. C.; Oakley, R. T.; Palstra, T. T. M.; Perel, A. S. *J. Am. Chem. Soc.* **1996**, *118*, 330. (f) Bryan, C. D.; Cordes, A. W.; Haddon, R. C.; Glarum, S. H.; Hicks, S. H.; Kennepohl, D. K.; MacKinnon, C. D.; Oakley, R. T.; Palstra, T. T. M.; Perel, A. S.; Schneemeyer, L. F.; Scott, S. R.; Waszczak, J. V. *J. Am. Chem. Soc*. **1994**, *116*, 1205. (g) Bryan, C. D.; Cordes, A. W.; Fleming, R. M.; George, N. A.; Glarum, S. H.; Haddon, R. C.; MacKinnon, C. D.; Oakley, R. T.; Palstra, T. T. M.; Perel, A. S. *J. Am. Chem. Soc.* **1995**, *117*, 6880. (h) Bryan, C. D.; Cordes, A. W.; George, N. A.; Haddon, R. C.; MacKinnon, C. D.; Oakley, R. T.; Palstra, T. T. M.; Perel, A. S. *Chem. Mater*. **1996**, *8*, 762.

(6) (a) Banister, A. J.; Bricklebank, N.; Lavender, I.; Rawson, J. M.; Gregory, C. I.; Tanner, B. K.; Clegg, W.; Elsegood, M. R. J.; Palacio, E. F. *Angew. Chem., Int. Ed. Engl.* **1996**, *35*, 2533. (b) Banister, A. J.; Bricklebank, N.; Clegg, W.; Elsegood, M. R. J.; Gregory, C. I.; Lavender, I.; Rawson, J. M.; Tanner, B. K. *J. Chem. Soc., Chem. Commun.* **1995**, 679.

(7) (a) Preston, K. F.; Sutcliffe, L. H. *Magn. Reson. Chem.* **1990**, *28*, 189. (b) Chung, Y.-L.; Fairhurst, S. A.; Gillies, D. G.; Preston, K. F.; Sutcliffe, L. H. *Magn. Reson. Chem.* **1992**, *30*, 666.

S0002-7863(97)03338-6 CCC: $15.00
Published on Web 01/01/1998

structural prescription for a neutral radical conductor.[4] Transport properties, however, have not been reported for this compound. A strongly slipped π-stack structure has recently been observed for the benzo-bridged diradical BBDTA **8**; variable temperature magnetic susceptibility and conductivity measurements indicate that the material is a small (0.2 eV) bandgap semiconductor.[13]

Recently, and as part of an exploration of the architectural issues behind the diverse structural patterns exhibited by DTA radicals, we reported the solid-state structures and magnetic properties of the 2,3-naphthalene- and quinoxaline-based derivatives NDTA **9** and QDTA **10**.[14] As a development of this work on NDTA and QDTA we have prepared and characterized the ternary heterocyclic radical 1,2,5-thiadiazolo[3,4-*b*]-1,3,2-dithiazolo[3,4-*b*]pyrazin-2-yl **11** (TDP-DTA). Measurement and

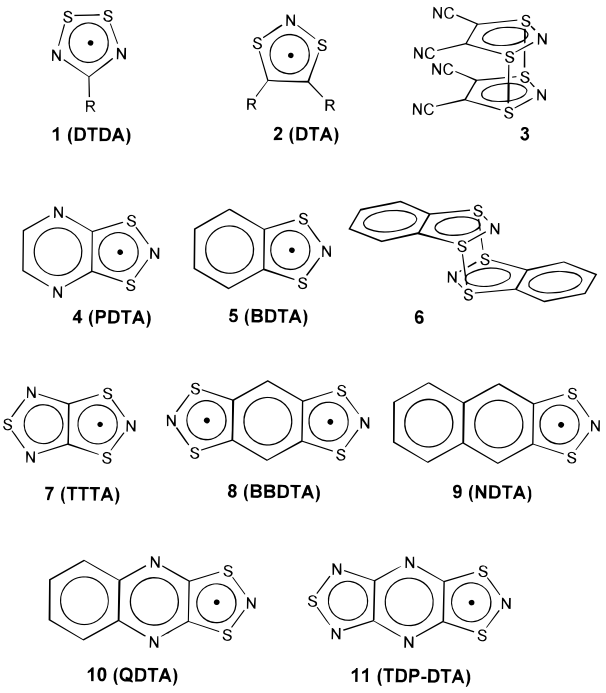

comparison of the electrochemical and ESR properties of all three radicals allows an interpretation of their transport properties in terms of the energetic and electronic criteria required for charge transport in a neutral radical conductor. Variable temperature magnetic susceptibility measurements on TDP-DTA have also been performed, and the nature of the observed phase transition near 150 K has been interpreted in the light of the results of single-crystal X-ray structure determinations at 293 and 150 K.

Scheme 1

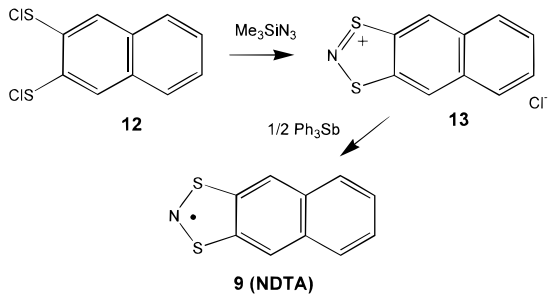

Scheme 2

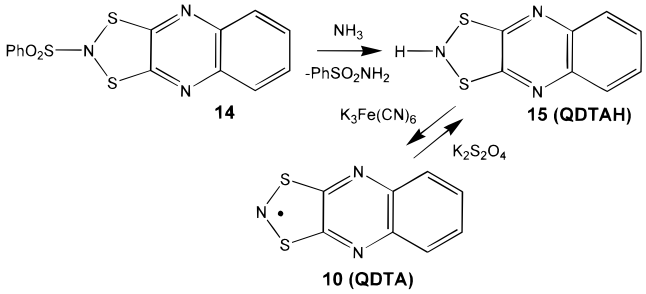

Results and Discussion

Preparation of Dithiazolyl Radicals. A variety of preparative routes to dithiazolyl radicals has been developed, and, as Wolmershäuser has pointed out,[10] there is no single method that serves for all systems. Most methods, indeed, have relatively restricted applicability. The reduction of dithiazolylium salts was one of the first approaches developed. The addition of the NS_2^+ cation to alkynes provides an effective route to the necessary dithiazolylium cations,[15] while the condensation of *ortho*-bis(sulfenyl chlorides) with trimethyl silyl azide allows access to aromatic derivatives such as BDTA[11] and BBDTA.[13] In this work we have employed the latter method to prepare NDTA. Thus the reaction of naphthalene-2,3-bis(sulfenyl chloride) **12**, itself prepared from the corresponding dithiol,[16] with trimethyl silyl azide leads to the dithiazolylium chloride [NDTA]Cl **13** (Scheme 1). We note that the preparation of the dithiol requires very stringent control of the oxidizing conditions; an excess of $PhICl_2$, or the use of more vigorous oxidants, e.g., chlorine, leads to chlorination of the aromatic ring. Reduction of [NDTA]Cl with triphenylantimony affords the neutral radical, which is extremely sensitive to atmospheric oxygen.

The preparation of QDTA, by the treatment of the corresponding benzenesulfonamide **14** Scheme 2) with ammonia, has been described by previous workers,[9] but in this work we have isolated and identified the necessary intermediate imide **15** (QDTAH). Oxidation of QDTAH with aqueous ferricyanide or molecular oxygen then affords the neutral radical QDTA. Blue solutions of QDTA in methylene chloride can be reduced to (yellow) QDTAH by treatment with aqueous dithionite. To our surprise attempts to extend this procedure to the synthesis of TDP-DTA failed. The necessary sulfonamide **16** cannot be prepared by the reaction of 5,6-dithiolo-1,2,5-thiadiazolo[3,4-

(8) (a) Awere, E. G.; Burford, N.; Mailer, C.; Passmore, J.; Schriver, M. J.; White, P. S.; Banister, A. J.; Oberhammer, A. J.; Sutcliffe, L. H. *J. Chem. Soc., Chem. Commun.* **1987**, 66. (b) MacLean, G. K.; Passmore, J.; Rao, M. N. S.; Schriver, M. J.; White, P. S. *J. Chem. Soc., Dalton Trans.* **1985**, 1405. (c) Wolmershäuser, G.; Kraft, G. *Chem. Ber.* **1989**, *122*, 385. (d) Harrison, S. R.; Pilkington, R. S.; Sutcliffe, L. H. *J. Chem. Soc., Faraday Trans. 1* 1984, *80*. 669. (f) Fairhurst, S. A.; Pilkington, R. S.; Sutcliffe, L. H. *J. Chem. Soc. Faraday Trans. 1* **1983**, *79*, 439. (g) Fairhurst, S. A.; Pilkington, R. S.; Sutcliffe, L. H. *J. Chem. Soc., Faraday Trans. 1* **1983**, *79*, 925.

(9) Wolmershäuser, G.; Kraft, G. *Chem. Ber.* **1990**, *123*, 881.

(10) Heckmann, G.; Johann, R.; Kraft, G.; Wolmershäuser, G. *Synth. Met.* **1991**, *41*−*43*, 3287.

(11) (a) Awere, E. G.; Burford, N.; Haddon, R. C.; Parsons, S.; Passmore, J.; Waszczak, J. V.; White, P. S. *Inorg. Chem.* **1990**, *29*, 4821. (b) Wolmershäuser, G.; Schnauber, M.; Wilhelm, T. *J. Chem. Soc., Chem. Commun.* **1984**, 573.

(12) Wolmershäuser, G.; Johann, R. *Angew. Chem., Int. Ed. Engl.* **1989**, *28*, 920.

(13) Barclay, T. M.; Cordes, A. W.; de Laat, R. H.; Goddard, J. D.; Haddon, R. C.; Jeter, D. Y.; Mawhinney, R. C.; Oakley, R. T.; Palstra, T. T. M.; Patenaude, G. W.; Reed, R. W.; Westwood, N. P. C. *J. Am. Chem. Soc.* **1997**, *119*, 2633.

(14) Barclay, T. M.; Cordes, A. W.; George, N. A.; Haddon, R. C.; Oakley, R. T.; Palstra, T. T. M.; Patenaude,G. W.; Reed,R. W.; Richardson, J. F.; Zhang, H. *J. Chem. Soc., Chem. Commun.* **1997**, 873.

(15) Parsons, S.; Passmore, J. *Acc. Chem. Res* **1994**, *27*, 101.

Scheme 3

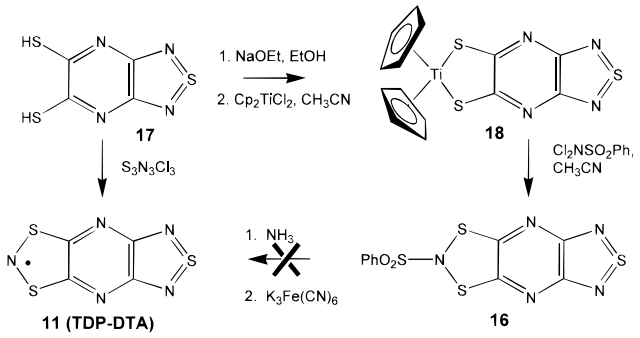

b]pyrazine **17** with benzene-*N*,*N*-dichlorosulfonamide but can be accessed by the preparation of the titanocene derivative **18** and its condensation with Cl_2NSO_2Ph (Scheme 3). However, treatment of the latter with ammonia leads not to the expected imide but rather to the recovery of benzene-sulfonamide and starting dithiol. While this route failed, we eventually discovered that TDP-DTA can be prepared, *in one step*, by treating the dithiol **17** with trithiazyl trichloride $S_3N_3Cl_3$. In the course of this reaction the chloride salt of the binary cation $S_4N_3^+$ is produced as a side product, along with the neutral (unoxidized) form of TDP-DTA. Under forcing conditions (excess chlorine gas) TDP-DTA can be oxidized to what we presume is a chloride salt of the corresponding dithiazolylium cation, but this material readily reverts to the neutral material (with loss of chlorine) upon heating it to 60 °C.

Cyclic Voltammetry. The most dramatic feature of the chemistry described above is the variation in redox properties along the series NDTA, QDTA, TDP-DTA. While NDTA reacts very rapidly with atmospheric oxygen, QDTA does not. Indeed QDTA is generated from its imide by treatment of the latter with oxygen. TDP-DTA is likewise quite resistant to oxidation, and chloride salts of the cationic state readily disproportionate on mild heating back to the neutral form (with loss of chlorine). To quantify these observations we have performed cyclic voltammetric (CV) measurements over the triad of oxidation states, i.e., anion, radical, and cation, available to these systems. The CV waves are illustrated in Figure 1, and the half-wave potentials for reduction and oxidation are summarized in Table 1, along with the values of E_{cell} ($E_{cell} = E_{1/2}(red) - E_{1/2}(ox)$). For all DTA radicals oxidation is essentially reversible. Electrochemical reduction of NDTA and QDTA is, however, strongly irreversible, as is the case for BDTA and BBDTA.[13] Only for TDP-DTA are both the oxidation and reduction steps reversible. Also presented in Table 1 are computed (MNDO) values for adiabatic ionization potentials (IPs) and electron affinities (EAs) as well as the difference IP − EA, i.e., the enthalpy change ΔH_{disp} for the gas-phase disproportionation reaction shown in eq 1. This parameter, which is the gas-phase analogue of E_{cell}, provides an indication of the Coulombic barrier to electron transfer in a neutral radical conductor.

$$2\ DTA \rightleftarrows DTA^+ + DTA^- \quad \Delta H_{disp} = (IP - EA) \quad (1)$$

It is immediately apparent that the electrochemical properties of NDTA, QDTA, and TDP-DTA parallel their chemical redox behavior. While NDTA is a remarkably powerful donor, rivalling, for example, TTF **19** ($E_{1/2}$ (ox) = 0.30 V vs SCE),[17] TDP-DTA is a strong acceptor, akin to closed shell heterocyclic

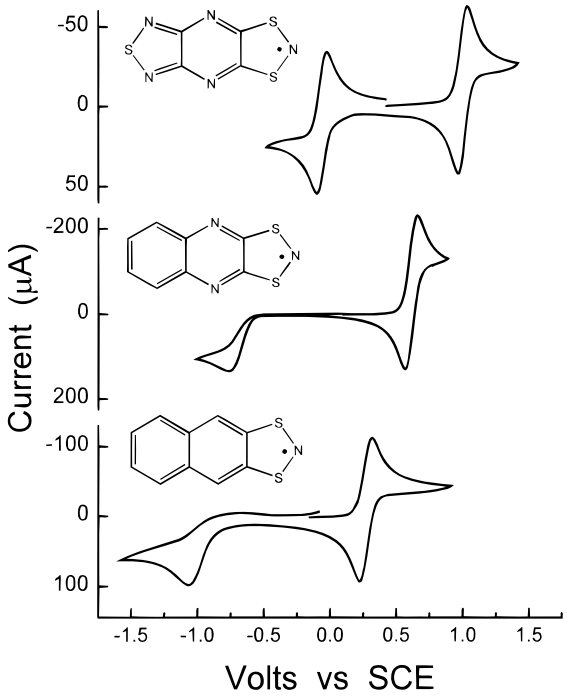

Figure 1. Cyclic voltammetry waves on NDTA, QDTA, and TDP-DTA radicals (in CH_3CN, *n*-Bu_4NPF_6 supporting electrolyte, ref SCE).

Table 1. Redox and E_{cell} Potentials[a] (volts vs SCE), Computed (MNDO) Adiabatic IP, and EA and ΔH_{disp} Values (eV) for 1,3,2-Dithiazolyls

compd	NDTA	QDTA	TDP-DTA
$E_{1/2}$(ox)	0.27	0.62	1.00
$E_{1/2}$(red)	−1.08[b]	−0.73[b]	−0.06
E_{cell}	1.29[c]	1.30[c]	1.06
IP	7.56	8.00	8.55
EA	1.71	2.18	3.02
ΔH_{disp}	5.85	5.84	5.53

[a] All potentals are from solutions in CH_3CN, reference SCE. [b] Irreversible. [c] This value is taken as the difference in the cathodic peak potentials, since the reduction wave is irreversible.

systems containing the thiadiazole unit, e.g., **20** ($E_{1/2}$ (red) = 0.10 V vs SCE).[18] This variation in redox potentials is in striking contrast to the behavior of DTDA radicals, where ligand effects

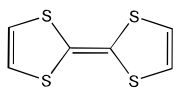

19

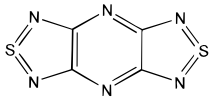

20

(at the 4-position) have relatively little influence on redox potentials,[19] ionization energies, and spin distributions.[20] Perhaps more notable, however, than the shift in potentials is the change in the value of E_{cell}, which drops markedly as the electron accepting ability of the heterocyclic residue attached to the DTA

(16) (a) Figuly, G. D.; Loop, C. K.; Martin, J. C. *J. Am. Chem. Soc.* **1989**, *111*, 654. (b) Block, E.; Eswarakrishnan, V.; Gernon, M.; Ofori-Okai, G.; Saha, C.; Tang, K.; Zubieta, J. *J. Am. Chem. Soc.* **1989**, *111*, 658. (c) Smith, K.; Lindsay, C. M.; Pritchard, G. J. *J. Am. Chem. Soc.* **1989**, *111*, 665.

(17) Lichtenberger, D. L.; Johnston, R. L.; Hinkelmann, K.; Suzuki, T.; Wudl, F. *J. Am. Chem. Soc.* **1990**, *112*, 3302.

(18) Yamashita, Y.; Saito, K.; Suzuki, T.; Kabuto, C.; Mukai, T.; Miyashi, T. *Angew. Chem., Int. Ed. Engl.* **1988**, *27*, 434.

(19) Boeré, R. T.; Moock, K. H. *J. Am. Chem. Soc.* **1995**, *117*, 4755.

(20) (a) Boeré, R. T.; Oakley, R. T.; Reed, R. W.; Westwood, N. P. C. *J. Am. Chem. Soc.* **1989**, *111*, 1180. (b) Cordes, A. W.; Goddard, J. D.; Oakley, R. T.; Westwood, N. P. C. *J. Am. Chem. Soc.* **1995**, *111*, 6147.

Table 2. ESR Hyperfine Coupling Constants *g*-Values, Hyperfine Coupling Constants a_N (mT) and Calculated (MNDO) Spin Densities q_N for 1,3,2-Dithiazolyls

compd	*g*	a_N[a]	q_N[a]
DTA, **2** (R = H)[b]	2.0071	1.066	0.459
BDTA, **5**	2.0069	1.101	0.464
TTTA, **7**[c]	2.0061	1.112 (0.084)	0.465 (0.039)
NDTA, **9**	2.0067	1.106	0.458
QDTA, **10**[d]	2.0065	1.089 (0.129)	0.456 (0.037)
TDP-DTA, **11**	2.0071	0.950 (0.207)	0.435 (0.060)

[a] Values in parentheses refer to the nitrogen atoms in the pyrazine ring. [b] Reference 7. [c] Reference 12. [d] Reference 9.

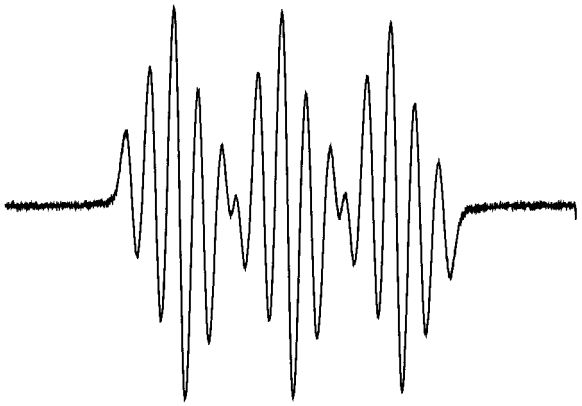

Figure 2. X-band ESR spectrum of TDP-DTA (in CH_2Cl_2, sweep width 0.50 mT).

ring is increased. The drop in E_{cell} is most pronounced for TDP-DTA. These experimental (solution) results are supported by the calculated (gas phase) disproportionation energies. The increase in IP along the series NDTA, QDTA and TDP-DTA is more than offset by the larger increase in EA in TDP-DTA, and the value of ΔH_{disp} drops by 0.3 eV. The implications of these results are elaborated below.

ESR Spectra. Values of the *g*-factors and isotropic hyperfine coupling constants a_N for NDTA, QDTA, TDP-DTA, and several related 1,3,2-dithiazolyl radicals are provided in Table 2,[7,21] along with computed (MNDO) estimates of the spin density q_N on nitrogen. For TDP-DTA the ESR spectrum itself is illustrated in Figure 2. All the radicals show the expected features for a 1,3,2-dithiazolyl radical, i.e., a large coupling to the nitrogen within the DTA ring. Taken together, however, the spectra reveal a progressive and significant decrease in this internal a_N value along the series NDTA, QDTA, and TDP-DTA. Coupled to this trend is a larger a_N value in the pyrazine ring of TDP-DTA (relative to QDTA). These experimental results follow closely the trends in computed spin densities. The singly occupied molecular orbital (SOMO) of TDP-DTA extends well out onto the pyrazine ring. In essence the thiadiazolopyrazine ring is an extremely effective sink for spin density, much more so than simple benzenoid aromatic residues, such as in BDTA or NDTA, or even simple thiadiazole units such as in TTTA.

Magnetic Susceptibility. The bulk magnetic properties of NDTA and QDTA were reported in an earlier communication.[14] In the solid state NDTA is essentially paramagnetic at room temperature, as expected from its herringbone packing pattern, which affords little opportunity for intermolecular exchange coupling. Upon cooling it undergoes two phase transitions, with eventual loss of paramagnetism. The slipped π-stack structure of QDTA leads to a room temperature magnetic susceptibility only 30% of that expected for a free spin system. Presumably this partial quenching reflects some intermolecular exchange

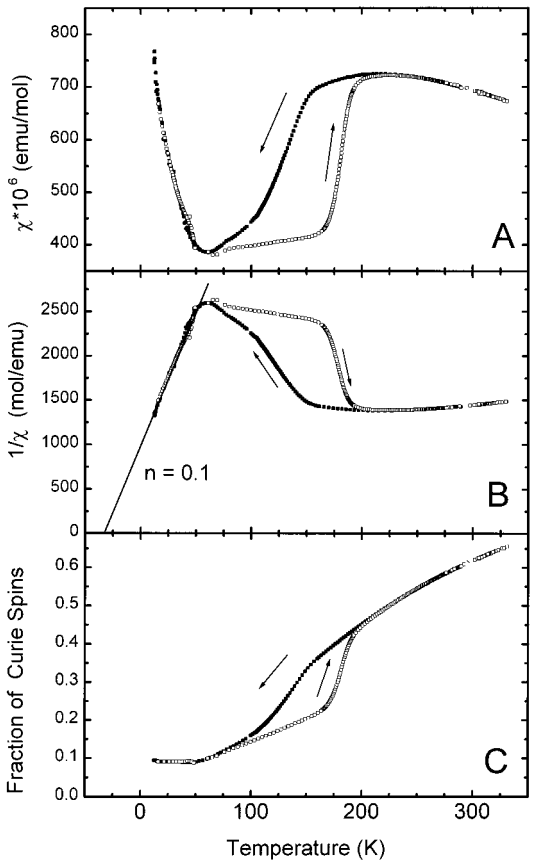

Figure 3. (A) Magnetic susceptibility χ of TDP-DTA as a function of temperature. (B) Plot of $1/\chi$ vs T for TDP-TDA. (C) Fraction of free Curie spins of TDP-DTA as a function of temperature.

interactions between the plates up and down the π-stack. Upon cooling the fraction of free spins slowly decreases, so that by 120 K all paramagnetism is quenched.

The results of magnetic susceptibility measurements on TDP-DTA, taken over the temperature range 4−330 K, are shown in Figure 3A. It is clear that there is a hysteretic phase transition in the vicinity of 150 K. In fitting the data we have used a calculated diamagnetic susceptibility correction of −92 ppm emu/mol. From the fit to the low-temperature data (Figure 3B) we obtain a Weiss constant for the ordering transition of about −34 K. This is the same order of magnitude as the hysteresis, and on this basis we assign the antiferromagnetic interaction as the origin of the phase transition. These two parameters have been used in Figure 3C to obtain the fraction of Curie spins as a function of temperature. It can be seen that Curie spins count is temperature dependent throughout the whole temperature range (down to near 50 K).

For the NDTA and QDTA systems the structural origins of the observed magnetic changes as a function of temperature in terms of variations in crystal structure were not investigated. While dimerization of some form provides a facile explanation for the loss of paramagnetism, the exact nature of how this process might occur is not known. In contrast to these to materials, the ground state of TDP-DTA is antiferromagnetic, and this unusual observation, coupled with the hysteretic phase transition observed in the region of 150 K, prompted us to explore the crystal structure of TDP-DTA above and below the phase transition observed in the magnetic measurements. The structural results are described below.

Crystal Structures. Although the compounds NDTA, QDTA, and TDP-DTA are similar at a molecular level, their

room-temperature solid-state structures are quite different. NDTA crystallizes as herringbone arrays,[14] like many polycyclic aromatics,[22] e.g., naphthalene[23] and anthracene,[24] while QDTA adopts a slipped π-stack structure[14] similar to that found for TTTA.[12] The different packing patterns exhibited by NDTA and QDTA provide a striking example of the effect of the presence, or absence, of CH---ring van der Waals interactions.[25] When such structure-making "tilted-T" contacts are possible, as in NDTA, then the well-known close-packed or herringbone arrangement is observed. When the opportunity for such interactions is reduced by CH/N replacement, as in QDTA, then a slipped π-stack structure prevails. In TDP-DTA there are no CH units at all, and extension of the previous argument would suggest a slipped π-stacked structure, as in QDTA and TTTA, or perhaps a stacked dimer structure, as in PDTA. As it turns out, both possibilities are correct.

We have investigated three crystal structures in the course of this work. That of compound **16**, the benzenesulfonamide derivative of TDP-DTA, was determined to establish the effect of substitution on ring planarity and to create bench mark bond lengths and angles for comparison with those of the radical (vide infra). The crystal structure consists of discrete molecules of **16**, with two molecules per asymmetric unit, differing primarily in the degree of torsion about the N−SO_2Ph bond. Both molecules, save for the substituted nitrogen atoms, are planar to within 0.085 Å, and the three-atom SNS envelope "flaps" make dihedral angles of 137.89(15)° and 143.17(15)° with the adjacent SCCS planes. These features are similar to that found in the toluenesulfonamide of 4,5-dicyano-DTA.[9]

The crystal structure of TDP-DTA, based on material grown by fractional sublimation at 110−60 °C/10^{-2} Torr, has been determined at both 293 and 150 K. These two temperatures are respectively above and below the phase transition observed in the magnetic measurements. While crystal selection and data collection at 293 K was a relatively simple task, characterization of the low temperature phase was extremely difficult. In most cases the crystals fractured, often violently, upon cooling, and on those occasions when the crystal displayed a sufficient lifetime at low temperature to allow data collection, the intensity of the data was low in comparison to the room-temperature response. The best refinement, the one reported here, is from a partial data set ($\theta_{max} = 21.5°$) obtained from a crystal which fractured after 36 h at 150 K.

Information on the unit cells of the room and low temperature phases is provided in Table 3, atomic coordinates are listed in Table 4, and mean intramolecular bond distances are summarized in Table 5. At room temperature crystals of TDP-DTA belong to the triclinic space group $P\bar{1}$, with two radicals per unit cell. The space group remains unchanged at 150 K, but the unit cell is dramatically different, containing two *dimeric* units. At 150 K there are three interannular S---S contacts, all of which are greater than 3.4 Å. As such these contacts are significantly longer than the interannular S---S "bonds" in other DTA dimers, e.g., **3** and **6**, and fall perilously close to the van der Waals separation for two sulfurs (3.6 Å).[26] Interestingly, of the three distances the shortest is between the two "tail" sulfurs (S_C---S_C in Table 5, i.e., S3 and S31 in Table 4). Dimerization has virtually no effect on the bonds within individual molecules; the bond lengths in the low- and high-temperature structures are almost identical. Dimerization does not lead to any significant puckering of either of the molecular halves, both of which remain planar to within 0.05 Å. The structural differences observed between TDP-DTA and its sulfonamide derivative **16** are largely restricted to the dithiazolyl ring and follow the pattern expected upon reduction of any 1,3,2-

Table 3. Crystal Data for 16 and TDP-DTA 11

compd	**16**	TDP-DTA	TDP-DTA
formula	$S_4O_2N_5C_{10}H_5$	$S_3N_5C_4$	$S_6N_{10}C_8$
fw	355.42	214.26	428.52
a, Å	10.2388(8)	4.4456(8)	7.489(7)
b, Å	11.8299(9)	8.407(2)	9.593(4)
c, Å	13.1024(12)	9.671(3)	10.759(6)
α, deg	115.066(7)	71.34(2)	65.77(4)
β, deg	94.083(8)	89.28(2)	74.10(6)
γ, deg	108.405(6)	87.80(2)	74.64(6)
V, Å^3	1324.7(2)	342.2(1)	667.5(9)
space group	$P\bar{1}$	$P\bar{1}$	$P\bar{1}$
Z	4	2	2
temp, K	293	293	150
μ, mm^{-1}	0.70	0.98	1.04
data with $I > n\sigma(I)$	5484 ($n = 0$)	1425 ($n = 2.5$)	1364 ($n = 2.5$)
parameters refined	380	110	97
$R(F)$, $R_w(F)$[a]	0.050, 0.052	0.032, 0.055	0.111, 0.137

[a] $R = [\sum||F_o| - |F_c||]/[\sum|F_o|]$; $R_w = \{[\sum w||F_o| - |F_c||^2]/[\sum(w|F_o|^2)]\}^{1/2}$.

Table 4. Atomic Parameters *x*, *y*, *z* and B_{iso} for TDP-DTA

$T = 293$ K				
	x	*y*	*z*	B_{eq}[a]
S1	0.82686(11)	0.53386(5)	0.17330(5)	2.849(18)
S2	1.05427(9)	0.29869(5)	0.42462(4)	2.335(16)
S3	0.22142(9)	−0.12463(5)	0.17519(4)	2.145(15)
N1	0.4998(3)	0.3019(2)	0.1116(1)	2.27(5)
N2	0.7509(3)	0.0523(2)	0.3736(1)	2.11(5)
N3	1.0400(4)	0.4939(2)	0.3177(2)	2.83(6)
N4	0.2327(3)	0.0744(2)	0.0846(1)	2.21(5)
N5	0.4537(3)	−0.1393(2)	0.3063(1)	2.32(5)
C1	0.6934(4)	0.3358(2)	0.2000(2)	1.97(5)
C2	0.4269(3)	0.1383(2)	0.1552(1)	1.85(5)
C3	0.5523(3)	0.0145(2)	0.2842(1)	1.80(5)
C4	0.8156(3)	0.2126(2)	0.3304(1)	1.86(5)
$T = 150$ K				
	x	*y*	*z*	B_{iso}
S2	0.5750(4)	0.2323(3)	0.1845(3)	1.20(7)
S1	0.3523(4)	0.2205(3)	0.4392(3)	1.03(7)
S3	0.5611(4)	0.8819(3)	0.1939(3)	0.99(7)
S21	0.1045(4)	0.3750(3)	0.1413(3)	1.08(7)
S11	−0.1122(4)	0.3579(3)	0.3987(3)	1.11(7)
S31	0.1025(4)	1.0177(3)	0.1592(3)	0.97(7)
N2	0.623(1)	0.524(1)	0.1220(9)	0.8(2)
N1	0.386(1)	0.512(1)	0.3907(9)	0.9(2)
N3	0.455(1)	0.132(1)	0.3315(9)	1.2(2)
N5	0.645(1)	0.776(1)	0.0992(9)	1.0(2)
N4	0.443(1)	0.766(1)	0.3269(9)	1.1(2)
N11	−0.074(1)	0.646(1)	0.3565(9)	1.2(2)
N21	0.160(1)	0.663(1)	0.0856(9)	1.2(2)
N31	−0.025(1)	0.276(1)	0.2843(10)	1.1(2)
N41	−0.017(1)	0.902(1)	0.2917(9)	1.2(2)
N51	0.186(1)	0.913(1)	0.0636(9)	1.1(2)
C4	0.544(2)	0.405(1)	0.2124(11)	0.9(2)
C3	0.582(2)	0.643(1)	0.1684(11)	1.1(2)
C2	0.463(2)	0.639(1)	0.3019(11)	0.8(2)
C1	0.425(2)	0.396(1)	0.3472(11)	0.9(2)
C11	−0.034(2)	0.533(1)	0.3083(11)	0.9(2)
C21	0.007(2)	0.771(1)	0.2649(11)	0.8(2)
C31	0.122(2)	0.780(1)	0.1328(11)	0.8(2)
C41	0.079(2)	0.543(1)	0.1737(11)	0.8(2)

[a] B_{eq} is the mean of the principal axes of the thermal ellipsoid.

(21) Chung, Y.-L.; Sandall, J. P. B.; Sutcliffe, L. H.; Joly, H.; Preston, K. F.; Johann, R.; Wolmershäuser, G. *Magn. Reson. Chem.* **1991**, *31*, 625.
(22) Gavezzotti, A.; Desiraju, G. R. *Acta Crystallogr.* **1988**, *44B*, 427.
(23) Dunitz, J. D.; Brock, C. P. *Acta Crystallogr.* **1982**, *38B*, 2218.
(24) Brock, C. P.; Dunitz, J. D. *Acta Crystallogr.* **1990**, *46B*, 795.
(25) Hobza, P.; Selzle, H. L.; Schlag, E. W. *J. Am. Chem. Soc.* **1994**, *116*, 3500.
(26) Bondi, A. *J. Phys. Chem.* **1964**, *68*, 441.

Table 5. Mean Structural Parameters (Å) in 16 and TDP-DTA 11[a,c]

	16	TDP-DTA	TDP-DTA
T, K	293	293	150
N_A-S_A	1.73(3)	1.636(3)	1.627(14)
S_A-C_A	1.755(16)	1.728(2)	1.73(3)
C_A-C_A	1.467(6)	1.448(2)	1.45(2)
C_A-N_B	1.297(3)	1.320(2)	1.319(14)
N_B-C_C	1.368(4)	1.356(3)	1.357(15)
C_C-C_C	1.424(4)	1.447(2)	1.44(3)
C_C-N_C	1.333(10)	1.334(4)	1.33(4)
N_C-S_C	1.620(2)	1.620(8)	1.614(17)
S_A---S_A			3.48(5)[b]
S_C---S_C			3.401(5)[b]

[a] Numbers in parentheses are the greater of the range or ESD. [b] Intradimer contacts. [c] Atoms grouped by ring as shown below. Ring labeling scheme:

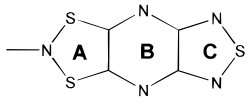

dithiazolyl, notably a lengthening of the S−N and S−C bonds.[13] That bond length changes extend into the pyrazine ring provides additional evidence for the extent of delocalization of the SOMO in TDP-DTA.

Figure 4 provides several views of the packing of TDP-DTA at 293 and 150 K. Both structures consist of ribbons of radicals (or dimers) layered into slipped π-stacks not unlike those found in QDTA; only the degree of slippage is more marked in the present case. At 293 K the lateral slippage between adjacent layers is such that equivalent atoms are separated by 4.454(1) Å, i.e., the unit cell repeat. In the 150 K structure slippage of the dimeric units is similar. For example, the tail sulfur (S_C) of one dimer is 4.556(5) Å from the tail sulfur (S_C) in the dimer above it. Outside of the intradimer S---S contacts already noted there are several short intermolecular (head-to-tail) S---S interactions (3.350(5) and 3.357(5) Å).

The association of TDP-DTA radicals at low temperature is not, in itself, a novel finding. Spin pairing by dimerization, i.e., covalent bond formation, is the fate of most sterically unencumbered radicals. What is interesting in the present system is the fact that the association does *not* lead to a complete quenching of paramagnetism. Also of interest is the mechanism of the phase transition; how do the two structures interconvert?

In the many DTDA systems which we have studied, the π-stacking of plates has been almost invariably superimposable. Dimerization requires little more than the coupling of the lattice to a charge density wave parallel to the stacking direction, so as to produce the characteristic oscillation in interplanar spacing along the stack.[5] In slipped π-stacks such as TDP-DTA dimerization requires displacive motion of layers of molecules across the stacking direction rather than along it. The abrupt, almost explosive fracturing of single crystals of TDP-DTA upon rapid cooling is reminiscent of the so-called "jumping crystal" phenomenon described by others.[27] Literature precedent for plate slippage interconversions in molecular crystals are, however, few. The closest analogy that we have found is the so-called martensitic[28,29] phase transition observed in *ttatt*-perhydropyrene.[30]

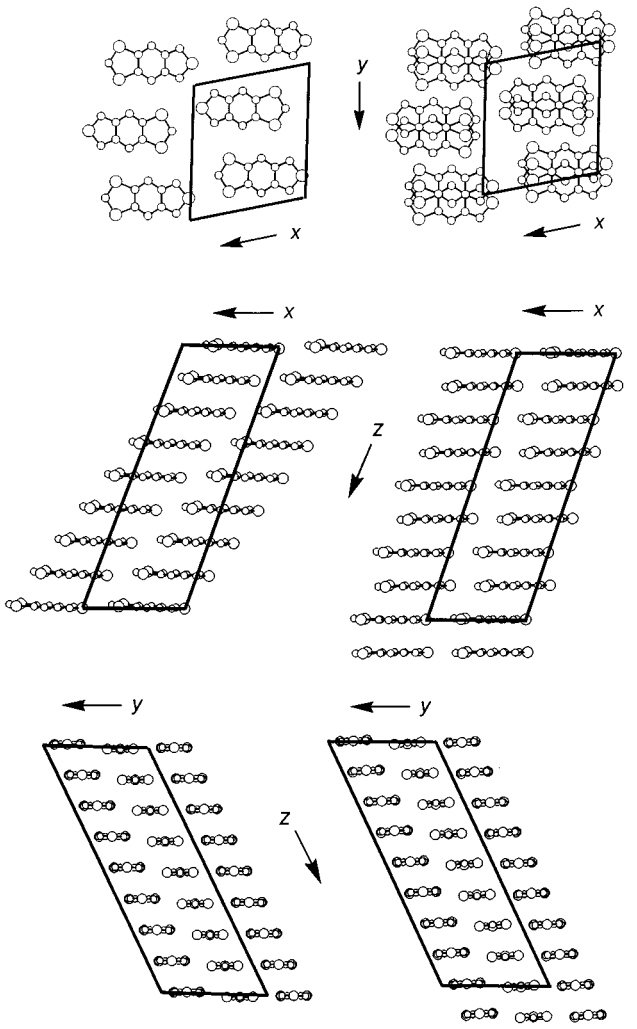

Figure 4. Three views of the TDP-DTA packing at 293 K (left) and 150 K (right). Above: sheets of radicals/dimers. Center: ribbons of radicals/dimers. Bottom: end-on view of ribbons. Supercells (see Table 6) are shown with heavy lines.

Our suggested mechanism for the structural interchange in TDP-DTA is built on the premise that lateral displacement or slippage of molecules within the crystals is reversible,[31] as implied by the magnetic behavior, and that the crystal symmetry is maintained throughout the phase transition. Accordingly the interconversion of the two structures can be envisaged as taking place within the confines of a common $P\bar{1}$ supercell. Analysis of the separate lattices for the two phases of TDP-DTA reveals two similar supercells comprised of eight layers of the 293 K structure and four layers of the 150 K structure. The dimensions of these cells are listed in Table 6 and illustrated in Figure 4. Individual layers, or plates, within the *xy* plane of these supercells experience very little internal reorganization, indeed the *a* and *b* vectors and the associated γ angle are virtually identical. To a first approximation, conversion of the room-temperature lattice into the low-temperature structure can be envisaged as taking place by a series of lateral displacements of these layers along the *x* direction, in a tectonic platelike fashion. The relative motion of the plates can be understood with reference to the simplified representation shown in Figure

(27) Dunitz, J. D.; Bernstein, J. *Acc. Chem. Res* **1995**, *28*, 193.
(28) Smallman, R. E. *Modern Physical Metallurgy*, 3rd ed.; Butterworth: London, 1970.
(29) Etter, M. C.; Siedle, A. R. *J. Am. Chem. Soc.* **1983**, *105*, 641.
(30) Ding, J.; Herbst, R.; Praefcke, K.; Kohne, B.; Saenger, W. *Acta Crystallogr.* **1991**, *47B*, 739.
(31) (a) Décoret, C. *Molecules Phys. Chem. Biol.* **1988**, *1*, 159. (b) Megaw, H. D. *Crystal Structures, a Working Approach*, W. B. Saunders Co.: London, 1973.

Table 6. Supercell Vectors[a] and Dimensions[b] for TDP-DTA

	293 K	150 K
a	9.660(2) [1$\bar{1}$0]	9.593(4) [0$\bar{1}$0]
b	11.408(4) [$\bar{1}\bar{1}$1]	11.300(4) [$\bar{1}$01]
c	31.923(6) [7$\bar{1}$0]	29.96(3) [$\bar{4}$00]
α	118.78(2)	113.70(5)
β	75.68(2)	74.64(5)
γ	77.23(2)	77.57(3)

[a] Supercell vectors expressed relative to standard cell. [b] The values of *a*, *b*, and *c* are in Å; α, *β* and *γ* are in deg.

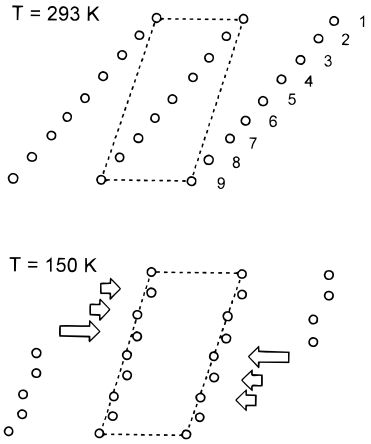

Figure 5. Qualitative views of the two phases of TDP-DTA, illustrating the direction and magnitude of "tectonic plate"slippage during the phase transition. The common supercell is shown with dashed lines.

5. Accordingly layers 2, 3, and 4 all shift in the same direction but to different extents. The largest shift (over 4 Å) is for layer 4. The motion of layers 5, 6, and 7 mirror these movements but in the opposite sense (Figure 5), i.e., a large shift for layer 5, with smaller shifts for layers 6 and 7. Insofar as these shifts are in opposite directions, the strain on the structure from the associated sheer forces between layers 4 and 5 must be considerable; the process amounts to a microscopic earthquake! It is not surprising, therefore, that crystals of TDP-DTA tend to shatter easily on cooling, as internal strain builds up in the high temperature structure and then is suddenly released. The hysteresis in the magnetic measurements can likewise be attributed to this kinetic effect. That the phase transition failed to occur (at 150 K) on one occasion underscores the importance of structural defects in acting as nucleation sites.

While the one-dimensional model for the motion of layers is conceptually appealing, it is incomplete. The discrepancy in the magnitude of the supercell *c* vectors, and the α angles, signals "tectonic plate" motion in the *y* direction as well as along *x*. The extent of motion along *y* is, however, much smaller than along *x*. A refinement of the supercell model, made by doubling the supercell from 8 to 16 layers, produces discrepancies in *c* and α of similar magnitude, but opposite sign. Clearly, an even larger supercell is required for a perfect match, but the conclusions of such a treatment would not differ qualitatively from those resulting from the simple eight-layer model presented here.

Summary and Conclusions

A range of synthetic methods now exists for the attachment of the 1,3,2-DTA radicals to organic and heterocyclic frameworks. In contrast to the behavior of 1,2,3,5-DTDA radicals, the redox chemistry of the DTA residue is markedly dependent on the donor/acceptor properties of the rest of the molecule. The shift in reduction potentials between NDTA and TDP-DTA is over 1 V. More importantly the attachment of extremely electron withdrawing substituents, as in TDP-DTA, leads to a decrease in the cell potential corresponding to the disproportionation of the radical. This decrease can be related to a lower barrier to charge transport between radical centers in the solid state and augurs well for the use of DTA derivatives in the design of single component neutral radical conductors. The crystal structure of TDP-DTA at 298 K consists of slipped *π*-stacks. However, while this configuration formally fulfills the structural criteria for a neutral *π*-radical conductor, i.e., evenly spaced plates, charge correlation effects still outweigh the electronic stabilization afforded by interannular orbital overlap, and the material remains a Mott insulator, with a pressed pellet conductivity $<10^{-6}$ S cm^{-1}. It is not difficult, however, to imagine more extended heterocyclic frameworks in which the ΔH_{disp} is further diminished by increasing the value of EA, and we are certainly pursuing the design and synthesis of such materials. An electronegative molecular metal, akin to the polymer $(SN)_x$,[32] may be possible. The major solid-state reorganization that accompanies the dimerization of TDP-DTA represents, to our knowledge, the first full characterization of such a process for a slipped *π*-stack structure. While the magnetic susceptibility changes that accompany the phase change, i.e., the reduction in free spins, are clearly understandable in terms of the observed solid-state rearrangement, it is noteworthy that some paramagnetism persists after dimerization and that the structure is a ground state antiferromagnet. This observation suggests that the intermolecular resonance interaction between the radical halves of the dimer is extremely weak, comparable to the magnitude of the exchange interaction between the two unpaired electrons. The implications of this possibility are currently being pursued.

Experimental Section

General Procedures and Starting Materials. Ammonia (Matheson), chloropyrazine (Aldrich), dichloroquinoxaline (Aldrich), naphthalene-2-thiol (Aldrich), bis(cyclopentadienyl)titanium dichloride (Aldrich), thiourea, iodobenzene, benzenesulfonamide (Aldrich), potassium ferricyanide (Aldrich), trimethylsilyl azide (Aldrich), triphenylantimony (Aldrich), silver powder (Aldrich) were all reagent grade chemicals obtained commercially. The compounds tetrachloropyrazine,[33] 2,3-diamino-5,6-dichloropyrazine,[34] 5,6-dichloro-1,2,5-thiadiazolo[3,4-*b*]-pyrazine,[34] iodobenzene dichloride,[35] 5,6-dithiolo-1,2,5-thiadiazolo[3,4-*b*]pyrazine **17**,[36] naphthalene-2,3-dithiol,[16] trithiazyl trichloride ($S_3N_3Cl_3$),[37] and *N*,*N*-dichlorobenzenesulfonamide[38] were all prepared by standard literature procedures. 1,3,2-Dithiazolo[4,5-*b*]quinoxaline-2-benzensulfonamide was also prepared as described,[9] but was recrystallized before use from chlorobenzene as yellow needles, mp 210−213 °C. Solvents were of reagent grade and dried by distillation from P_2O_5 (for CH_3CN and CH_2Cl_2), Na (for toluene), and Mg (for EtOH). Crystals for X-ray work were grown by sublimation in an ATS series 3210 three-zone tube furnace mounted horizontally and linked to a series 1400 temperature control system. Melting points are uncorrected. ^{1}H and ^{13}C NMR spectra were recorded on a Varian Gemini 200 MHz NMR or a Varian Unity 400 MHz NMR spectrometer; chemical shift values were internally referenced to TMS or to the residual proton signals of the solvent (*δ*, C*H*Cl$_3$). Infrared spectra (Nujol mulls, KBr optics) were recorded on a Nicolet 20SX/C FTIR spectrometer at 2 cm^{-1} resolution.

(32) Labes, M. M.; Love, P.; Nichols, L. F. *Chem. Rev.* **1979**, *1*, 79.
(33) Allison, C. G.; Chambers, R. D.; MacBride, J. A. H.; Musgrave, W. K. R. *J. Chem. Soc. C* **1970**, 1023.
(34) Tong, Y. C. *J. Heterocycl. Chem.* **1975**, *12*, 451.
(35) Lucas, H. J.; Kennedy, E. R. *Organic Syntheses*; Wiley: New York, 1955; Collect. Vol. 3, p 482.
(36) Tomura, M.; Yamashita, Y. J. *Mater. Chem.* **1995**, *5*, 1753.
(37) Alange, C. G.; Banister, A. J.; Bell, B. *J. Chem. Soc., Dalton Trans.* **1972**, 2399.
(38) Akiyoshi, S.; Okuno, K. *J. Am. Chem. Soc.* **1954**, *76*, 693.

Low resolution mass spectra (70 eV, EI) were obtained on a Kratos MS890 spectrometer using direct probe inlet techniques. X-Band ESR spectra were recorded on a Varian E−109 spectrometer with DPPH as a field marker. Elemental analyses were performed by MHW Laboratories, Phoenix, AZ 85018.

Preparation of Naphthalene-2,3-bis(sulfenyl chloride). Freshly prepared iodobenzene dichloride (4.88 g, 17.8 mmol) was slowly added portionwise to a stirred solution of naphthalene-2,3-dithiol (1.55 g, 8.1 mmol) in 50 mL of CH_2Cl_2 at 0 °C, and the resulting mixture allowed to warm slowly (2 h) to room temperature. The solvent was then removed in vacuo from the filtrate to leave a yellow crystalline solid that was recrystallized from 15 mL CH_3CN to give naphthalene-2,3-bis(sulfenyl chloride) (1.62 g, 6.2 mmol, 77%), mp 90−93 °C. IR (1600−400 cm^{-1}) 1618 (w), 1569 m), 1311 (w), 971 (w), 899 (w), 880 (s), 770 (w), 755 (vs), 722 (w), 470 (s) cm^{-1}. ^1H NMR (δ, $CDCl_3$) 8.1 (s, 2H), 7.85 and 7.55 (AA′BB′, 4H). Anal. Calcd for $C_{10}H_6NS_2Cl_2$: C, 45.99, H, 2.32; Cl, 27.15. Found: C: 46.17; H, 2.40; Cl, 27.40.

Preparation of Naphthalene-2,3-(1,3,2-dithiazolyl) NDTA. A solution of trimethylsilyl azide (0.55 g, 4.8 mmol) in 10 mL of CH_2Cl_2 was added dropwise to a stirred solution of naphthalene-2,3-bis(sulfenyl chloride) (1.2 g, 4.6 mmol) in 40 mL CH_2Cl_2. Slow effervescence of N_2 was observed, and the solution changed to a dark red color. A cherry red precipitate of naphthalene-2,3-(1,3,2-dithiazolylium chloride) was also produced. After 2 h the solid was filtered off, washed with 2 × 20 mL CH_2Cl_2, and dried in vacuo. IR (1600−400 cm^{-1}) 1557 (w), 1350 (w), 1323 (w), 1264 (m), 1154 w), 1073 (m), 965 (w), 883 (s), 801 (w), 783 (m), 750 (s), 601 (w), 551 9w), 429 (w), 477 (m), 429 (m) cm^{-1}. This crude salt was slurried in 60 mL of CH_3CN and reduced by the addition of a solution of triphenylantimony (0.81 g, 2.3 mmol) in 10 mL CH_3CN at 0 °C. After 1 h the crude product was filtered off and dried in vacuo. Purification was effected by fractional sublimation at 80−50 °C/10^{-2} Torr, to afford purple plates of NDTA **9** (0.28 g, 1.4 mmol, 30% based on bis(sulfenyl chloride)), mp 149−50 °C. IR (1600−400 cm^{-1}) 1315 (w), 1269 (w), 127 (w), 1195 (w), 874 (vs), 767 (s), 700 (s), 693 (m), 480 (m), 470 (w) cm^{-1}. MS (*m*/*z*): 204 (M^+, 100%), 158 ([M-NS]$^+$, 15%), 140 (6%), 114 (11%), 102 12%), 69 (4%). Anal. Calcd for $C_{10}H_6NS_2$: C, 58.80, H, 2.96; N, 6.86. Found: C, 59.03; H, 3.12; N, 6.83.

Preparation of 1,3,2-Dithiazolo[4,5-*b*]quinoxaline QDTAH. Anhydrous ammonia was gently bubbled through a slurry of sulfonamide **14** (2.00 g, 5.76 mmol) in 100 mL of CH_2Cl_2 held at 0 °C, to produce an off-white gelatinous precipitate in a green solution. After 15 min the gas flow was halted, and the precipitate of benzenesulfonamide filtered off. The solvent was removed in vacuo from the filtrate, and the residual solid extracted with 100 mL of warm toluene (under nitrogen). The mixture was again filtered (to remove residual benzenesulfonamide), and the solvent was again removed in vacuo. The yellow green product (0.91 g, 4.4 mmol, 76%) was recrystallized from hot ethanol as pale yellow needles of QDTAH **15**, dec 122−24 °C. IR: ν(NH) 3168 cm^{-1} and (1600−400 cm^{-1}) 1559 (w), 1247 (w), 1161 (m), 1130 (w), 1092 (m), 1016 (w), 1008 (w), 932 (m), 770 (m), 757 (s), 669 (w), 643 (m), 595 (m), 466 (w), 412 (m) cm^{-1}. ^1H NMR (δ, $CDCl_3$): 4.89 (s, NH), 7.62 and 7.86 (AA′BB′, 4H). MS (*m*/*z*): 206 (M^+, 100%,), 160 ([M − NS]$^+$, 61%), 102 (33%), 77 (21%), 51(18%). Anal. Calcd for $C_8H_5N_3S_2$: C, 46.36, H, 2.43; N, 20.27. Found: C, 46.53; H, 2.27, N, 20.06.

Preparation of 1,3,2-Dithiazolo[4,5-*b*]quinoxalin-2-yl QDTA. Crude QDTAH, prepared as described above from the sulfonamide (2.18 g, 6.3 mmol), was dissolved in 100 mL of CH_2Cl_2, the solution was treated with a solution of potassium ferricyanide (2.0 g, 6.1 mmol) in 100 mL of H_2O, and the two-phase mixture was vigorously stirred for 8 h. The dark blue organic layer was then separated, dried over sodium sulfate, and evaporated to dryness to leave QDTA **10** as a blue/black crystalline solid (1.0 g, 4.8 mmol, 77% from sulfonamide). The product was purified by fractional sublimation over the range 90−45 °C/10^{-2} Torr to yield black needles, mp 137−140 °C (lit. 132 °C[9]).

Preparation of $TDPS_2TiCp_2$ 18. Solid **17** (1.50 g, 7.4 mmol) was added to a solution of sodium ethoxide prepared from sodium (0.34 g, 14.8 mmol) and anhydrous ethanol (30 mL). The resulting slurry was stirred under N_2 for 90 min, and then the solid filtered off and dried in vacuo to yield the crude red-brown disodium salt (1.70 g, 6.9 mmol). This solid was added to 100 mL of CH_3CN, and finely powdered Cp_2TiCl_2 (1.72 g, 6.9 mmol) was slowly added to the stirred mixture. The red-brown solid was slowly converted into a dark green solid. After 15 h the crude product was filtered off, and Soxhlet extracted exhaustively (72 h) with CH_2Cl_2. Addition of toluene to the extracts and slow rotary evaporation of the dark green solution afforded green black microcrystals of $TDPS_2TiCp_2$ **18** (1.06 g, 2.8 mmol, 42%), mp > 300 °C. IR (1600−400 cm^{-1}), 1379 (m), 1351 (m) 1309 (w), 1248 (w) 1114 (s), 1083 (br, w), 937 (br, w), 882 (m), 829 (br, s), 816 (m), 731 (br, w), 652 (m), 626 (w), 558 (w), 444 (w), 411 (m) cm^{-1}. Anal. Calcd for $C_{14}H_{10}N_4S_3Ti$: C, 44.45; H, 2.66; N, 14.81. Found: C, 44.61; H, 2.63, N, 14.48. ^1H NMR (δ, $CDCl_3$): 5.28 (s, 5H), 6.02 (s, 5H).

Preparation of Compound 16. *N*,*N*-Dichlorobenzenesulfonamide (0.39 g, 1.7 mmol) was added to a slurry of **18** (0.65 g, 1.7 mmol) in 75 mL of CH_3CN. The green solution immediately turned red-brown. After 2 h at room temperature the mixture was filtered, and the filtrate evaporated to dryness in vacuo to leave a mixture Cp_2TiCl_2 (red) and a yellow crystalline material. This mixture was extracted with 50 mL of warm toluene and the extract evaporated to leave a solid which was dissolved in 50 mL of warm CH_3CN. The solution was then cooled to 0 °C overnight. Subsequent filtration afforded yellow needles of the benzenesulfonamide **16** (0.30 g, 0.80 mmol, 49%), mp 184−86 °C. Transparent yellow blocks suitable for X-ray work were grown by sublimation at 130−80 °C/10^{-2} Torr. IR (1600−400 cm^{-1}): 1582 (w), 1403 (w), 1324 (w), 1313 (w), 1296 (w), 1250 (w), 1195 (w), 1175 (s), 1112 (s), 1083 (m), 1024, 1002 (w), 943 (w), 908 (w), 1175 (s), 1171 (s), 1129 (m), 818 (m) 813 (m), 781 (s), 757 (s), 726 (s), 689 (s), 637 (m), 599 (s), 569 (s), 549 (s), 494 (w), 472 (m), 424 (w) cm^{-1}. MS (EI, *m*/*e*): 355 (M^+, 16%), 291 ([M − SO_2]$^+$, 8%), 214 ([M − SO_2Ph]$^+$, 100%), 141 (SO_2Ph^+, 64%), 77 ($C_6H_5^+$, 100%). Anal. Calcd for $C_{10}H_5N_5O_2S_4$: C, 33.79; H, 1.42; N, 19.70. Found: C, 33.87; H, 1.44; N, 19.81.

Preparation of TDP-DTA. Solid $S_3N_3Cl_3$ (1.50 g, 6.1 mmol) was added to a slurry of the dithiol **17** (1.20 g, 5.9 mmol) in 50 mL of CH_3CN, and the mixture was heated at a gentle reflux for 4 h. The resulting mixture, a red solution and a dark brown solid, was filtered, and the solid dried in vacuo. IR analysis of this mixture revealed the presence of neutral TDP-DTA and the salt S_4N_3Cl (by comparison of its IR spectrum with that of a known sample[39]). The latter was removed by reducing the whole with excess Ph_3Sb (1.06 g, 3.0 mmol) in refluxing CH_3CN for 30 min (this effected the conversion of S_4N_3Cl to the more soluble S_4N_4). Hot filtration then afforded black microcrystals of TDP-DTA **11**, which were purified by fractional sublimation over the range 110−60 °C/ 10^{-2} Torr as lustrous black needles (0.56 g, 2.6 mmol, 44%) dec >186 °C. IR (1600−400 cm^{-1}), 1429 (w), 1379 (w), 1316 (br, m), 1246 (w), 1136 (w), 906 (w), 880 (m), 867 (m), 805 (s), 713, 694 (m), 665 (m), 641 (w), 534 (s), 503 (s), 426 (m) cm^{-1}. MS (EI, *m*/*e*): 214 (M^+, 85%, 1680 ([M − SN]$^+$, 7%), 78 (S_2N^+, 15%), 46 (SN^+, 100%). Anal. Calcd for $C_4N_5S_3$: C, 22.42; N, 32.69. Found: C, 22.91; N, 33.01.

Cyclic Voltammetry. Cyclic voltammetry on DTA radicals was performed on a PAR 273A electrochemical system (EG&G Instruments) with scan rates 50−100 mV s^{-1} on solutions of the radical (0.1 M tetra-*n*-butylammonium hexafluorophosphate) in CH_3CN. Potentials were scanned from −2.5 to 1.5 V with respect to the quasi-reference electrode in a single compartment cell fitted with Pt electrodes and referenced to the ferrocenium/ferrocene couple at 0.38 V vs SCE.[40]

X-ray Measurements. X-ray data were collected on ENRAF-Nonius CAD-4 diffractometers (at Arkansas and Louisville) with monochromated Mo Kα radiation. Crystals were mounted on glass fibers with silicone or epoxy. Data were collected using a $\theta/2\theta$ technique. The structures were solved using direct methods and refined by full-matrix least squares which minimized $\sum w(\Delta F)^2$.

Magnetic Susceptibility Measurements. Magnetic susceptibilities were measured over the temperature range 5−330 K on a George Associates Faraday balance operating at 0.5 T.

(39) Jolly, W. L.; Maguire, K. D. *Inorg. Syntheses* **1967**, *9*, 102.
(40) Boeré, R. T.; Moock, K. H.; Parvez, M. *Z. Anorg. Allg. Chem.* **1994**, *620*, 1589.

Electronic Structure Calculations. MNDO calculations were carried out on a Pentium 166 PC using the MOPAC93 suite of programs[41] compiled to run under DOS. All geometries were optimized within the constraints of C_{2v} symmetry. The potential for folding of the anion derivatives[13] was not explored. Spin densities q_N refer to the square of the pπ-orbital coefficients in the SOMO.

Acknowledgment. We thank the Natural Sciences and Engineering Research Council of Canada, the NSF/EPSCOR program, and the State of Arkansas for financial support. One of us (T.M.B.) acknowledges the Department of Education for a doctoral fellowship.

(41) MOPAC93, Quantum Chemistry Program Exchange.

Supporting Information Available: Tables of crystal data, structure solution and refinement, bond lengths and angles, and anisotropic thermal parameters for the structures reported (14 pages). See any current masthead page for ordering and Internet access instructions.

JA973338A